

## University of Massachusetts Boston ScholarWorks at UMass Boston

Physics Faculty Publications

Physics

6-20-2007

# Strain-free Ge/GeSiSn quantum cascade lasers based on L-valley intersubband transitions

Greg Sun

*University of Massachusetts Boston, [greg.sun@umb.edu](mailto:greg.sun@umb.edu)*

H. H. Cheng

*National Taiwan University*

J. Menéndez

*Arizona State University at the Tempe Campus*

Jacob B. Khurgin

*Johns Hopkins University*

R. A. Soref

*Air Force Research Laboratory, Hanscom Air Force Base*

Follow this and additional works at: [http://scholarworks.umb.edu/physics\\_faculty\\_pubs](http://scholarworks.umb.edu/physics_faculty_pubs)

 Part of the [Physics Commons](#)

### Recommended Citation

Sun, Greg; Cheng, H. H.; Menéndez, J.; Khurgin, Jacob B.; and Soref, R. A., "Strain-free Ge/GeSiSn quantum cascade lasers based on L-valley intersubband transitions" (2007). *Physics Faculty Publications*. Paper 20.

[http://scholarworks.umb.edu/physics\\_faculty\\_pubs/20](http://scholarworks.umb.edu/physics_faculty_pubs/20)

This Article is brought to you for free and open access by the Physics at ScholarWorks at UMass Boston. It has been accepted for inclusion in Physics Faculty Publications by an authorized administrator of ScholarWorks at UMass Boston. For more information, please contact [library.uasc@umb.edu](mailto:library.uasc@umb.edu).

## Strain-free Ge/GeSiSn quantum cascade lasers based on L-valley intersubband transitions

G. Sun, H. H. Cheng, J. Menéndez, J. B. Khurgin, and R. A. Soref

Citation: *Appl. Phys. Lett.* **90**, 251105 (2007); doi: 10.1063/1.2749844

View online: <http://dx.doi.org/10.1063/1.2749844>

View Table of Contents: <http://apl.aip.org/resource/1/APPLAB/v90/i25>

Published by the [American Institute of Physics](http://www.aip.org).

---

### Related Articles

Electroluminescence from strained germanium membranes and implications for an efficient Si-compatible laser  
*Appl. Phys. Lett.* **100**, 131112 (2012)

A weakly coupled semiconductor superlattice as a potential for a radio frequency modulated terahertz light emitter  
*Appl. Phys. Lett.* **100**, 131104 (2012)

Quantum-dot nano-cavity lasers with Purcell-enhanced stimulated emission  
*Appl. Phys. Lett.* **100**, 131107 (2012)

Effect of internal optical loss on the modulation bandwidth of a quantum dot laser  
*Appl. Phys. Lett.* **100**, 131106 (2012)

Design of three-well indirect pumping terahertz quantum cascade lasers for high optical gain based on nonequilibrium Green's function analysis  
*Appl. Phys. Lett.* **100**, 122110 (2012)

---

### Additional information on *Appl. Phys. Lett.*

Journal Homepage: <http://apl.aip.org/>

Journal Information: [http://apl.aip.org/about/about\\_the\\_journal](http://apl.aip.org/about/about_the_journal)

Top downloads: [http://apl.aip.org/features/most\\_downloaded](http://apl.aip.org/features/most_downloaded)

Information for Authors: <http://apl.aip.org/authors>

## ADVERTISEMENT

NEW!

iPeerReview

AIP's Newest App



Authors...  
Reviewers...

Check the status of  
submitted papers remotely!

AIP | Publishing

## Strain-free Ge/GeSiSn quantum cascade lasers based on *L*-valley intersubband transitions

G. Sun

*Department of Physics, University of Massachusetts Boston, Massachusetts 02125*

H. H. Cheng<sup>a)</sup>

*Center for Condensed Matter Sciences, National Taiwan University, Taipei, 106,*

*Taiwan and Graduate Institute of Electronics Engineering, National Taiwan University, Taipei 106, Taiwan*

J. Menéndez

*Department of Physics and Astronomy, Arizona State University, Tempe, Arizona 85287*

J. B. Khurgin

*Department of Electrical and Computer Engineering, Johns Hopkins University, Baltimore, Maryland 21218*

R. A. Soref

*Sensors Directorate, Air Force Research Laboratory, Hanscom AFB, Massachusetts 01731*

(Received 11 April 2007; accepted 24 May 2007; published online 20 June 2007)

The authors propose a Ge/Ge<sub>0.76</sub>Si<sub>0.19</sub>Sn<sub>0.05</sub> quantum cascade laser using intersubband transitions at *L* valleys of the conduction band which has a “clean” offset of 150 meV situated below other energy valleys ( $\Gamma, X$ ). The entire structure is strain-free because the lattice-matched Ge and Ge<sub>0.76</sub>Si<sub>0.19</sub>Sn<sub>0.05</sub> layers are to be grown on a relaxed Ge buffer layer on a Si substrate. Longer lifetimes due to the weaker scattering of nonpolar optical phonons reduce the threshold current and potentially lead to room temperature operation. © 2007 American Institute of Physics. [DOI: 10.1063/1.2749844]

Electrically pumped Si-based lasers have long been sought because they serve as light sources for monolithic integration of Si electronics with photonic components on the same Si wafer. Unfortunately, Si has not been a material of choice for luminescence applications owing to its indirect band gap. It has been proposed that lasers based on intersubband transitions (ISTs) in SiGe quantum wells (QWs) could circumvent the issue of band gap indirectness.<sup>1</sup> In addition, SiGe QWs, being a nonpolar material, are expected to have longer intersubband lifetimes that reduce the threshold current and to be free from the reststrahl absorption that is found in III-V quantum cascade lasers (QCLs). Various groups have obtained electroluminescence from Si-rich Si/SiGe quantum cascade structures,<sup>2–4</sup> but lasing has eluded researchers up to now. Those efforts all have one scheme in common: holes instead of electrons are used for IST because most of the band offset between the Si-rich SiGe QWs and the Si barriers is in the valence band. There are a number of difficulties associated with valence band Si/SiGe QCLs. First, the strong mixing of heavy-hole, light-hole, and split-off bands makes the QCL design exceedingly cumbersome and adds a great degree of uncertainty. Second, the large effective mass of heavy holes hinders carrier injection efficiency and leads to small IST oscillator strength between laser states. Third, for any significant band offset needed to implement QCLs, lattice-mismatch-induced strain in SiGe QWs is likely to limit total structural thickness in order to avoid generation of structural defects. Recently, a conduction intersubband approach was proposed to construct a Ge/SiGe QCL using strained Ge QWs and SiGe alloy barriers.<sup>5</sup> That structure effectively avoids the valence band complexity, but

the two  $\Delta_2$  valleys along the (001) growth direction are still entangled with the *L* valleys in the conduction band, leading to design complexity and potentially creating additional non-radiative decay channels for the upper laser state.

In this letter, we propose to employ Ge/Ge<sub>1-x-y</sub>Si<sub>x</sub>Sn<sub>y</sub> heterostructures to develop *L*-valley QCLs. Ge<sub>1-x-y</sub>Si<sub>x</sub>Sn<sub>y</sub> alloys have been studied for the possibility of forming direct band gap semiconductors.<sup>6–9</sup> Since the initial growth of this alloy,<sup>10</sup> device-quality epilayers with a wide range of alloy contents have been achieved. Incorporation of Sn provides the opportunity to engineer separately the strain and band structure since we can vary the Si (*x*) and Sn (*y*) compositions independently. Certain alloy compositions of this material system offer three advantages: (1) the possibility of a “cleaner” conduction band lineup in which the *L* valleys in both well and barrier sit below other valleys ( $\Gamma, X$ ), (2) an electron effective mass along the (001) growth direction that is much lower than the prior heavy-hole mass, and (3) a lattice-matched structure that is entirely strain-free. In addition, recent advances in the direct growth of Ge layer on Si provide a relaxed matching buffer layer on a Si substrate upon which the strain-free QCL is grown,<sup>11</sup> although precise control of the layer thickness and interface sharpness is yet to be accomplished before the proposed QCL can be implemented.

Since band offsets between ternary Sn-containing alloys and Si or Ge are not known experimentally, we have calculated the conduction band minima for a lattice-matched heterostructure consisting of Ge and a ternary Ge<sub>1-x-y</sub>Si<sub>x</sub>Sn<sub>y</sub> based on Jaros’ band offset theory,<sup>12</sup> which is in good agreement with experiment for many heterojunction systems. For example, this theory predicts an average valence band offset,  $\Delta E_{v,av} = 0.48$  eV for a Ge/Si heterostructure (higher energy

<sup>a)</sup>Electronic mail: hhcheng@ntu.edu.tw

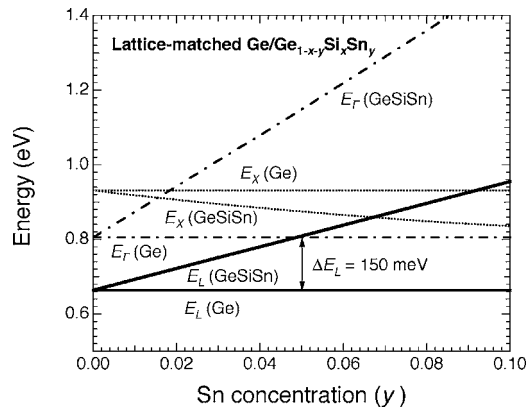


FIG. 1. Conduction band minima at  $L, \Gamma, X$  points of  $\text{Ge}_{1-x-y}\text{Si}_x\text{Sn}_y$  that is lattice matched to Ge.

on the Ge side), close to the accepted value of  $\Delta E_{v,av} = 0.5$  eV. The basic ingredients of our calculation are the average (between heavy, light, and split-off hole bands) valence band offset between the two materials and the compositional dependence of the band structure of the ternary alloy. For a Ge/ $\alpha$ -Sn interface Jaros' theory predicts  $\Delta E_{v,av} = 0.69$  eV (higher energy on the Sn side). For the  $\text{Ge}_{1-x-y}\text{Si}_x\text{Sn}_y/\text{Ge}$  interface we have used the customary approach for alloy semiconductors, interpolating the average valence band offsets for the elementary heterojunctions Ge/Si and Ge/ $\alpha$ -Sn. Thus we used  $\Delta E_{v,av}(x,y) = E_{v,av}(\text{GeSiSn}) - E_{v,av}(\text{Ge}) = -0.48x + 0.69y$  (in eV). Once the average valence band offset is determined, the energies of individual conduction band edges in the  $\text{Ge}_{1-x-y}\text{Si}_x\text{Sn}_y$  alloy can be calculated relative to those in Ge from the compositional dependence of the spin-orbit splitting of the top valence band states and the compositional dependence of the energy separations between those conduction band edges and the top of the valence band in the alloy.<sup>13</sup> We have assumed that all required alloy energies can be interpolated between the known values for Si, Ge, and  $\alpha$ -Sn as

$$E_{\text{GeSiSn}}(x,y) = E_{\text{Ge}}(1-x-y) + E_{\text{Si}}x + E_{\text{Sn}}y - b_{\text{GeSi}}(1-x-y)x - b_{\text{GeSn}}(1-x-y)y - b_{\text{SiSn}}xy. \quad (1)$$

The bowing parameters  $b_{\text{GeSi}}$ ,  $b_{\text{GeSn}}$ , and  $b_{\text{SiSn}}$  have been discussed in Refs. 14 and 15. Finally, for the indirect conduction band minimum near the  $X$  point, Weber and Alonso find  $E_X = 0.931 + 0.018x + 0.206x^2$  (in eV) for  $\text{Ge}_{1-x}\text{Si}_x$  alloys.<sup>16</sup> On the other hand, the empirical pseudopotential calculations of Cohen and Bergstresser place this minimum at 0.90 eV in  $\alpha$ -Sn, virtually the same as its value in pure Ge.<sup>17</sup> We thus assume that the position of this minimum in ternary  $\text{Ge}_{1-x-y}\text{Si}_x\text{Sn}_y$  alloys is independent of the Sn concentration  $y$ . This is qualitatively in agreement with the virtual-crystal calculations of Jenkins and Dow,<sup>7</sup> which find that the  $X$ -related minima have the weakest compositional dependence. The conduction band minima results are shown in Fig. 1 for Sn concentrations  $0 < y < 0.1$ . The Si concentration  $x$  was calculated using Vegard's law in such a way that the ternary  $\text{Ge}_{1-x-y}\text{Si}_x\text{Sn}_y$  is exactly lattice matched with Ge.

It can be seen from Fig. 1 that a conduction band offset of 150 meV at  $L$  valleys can be obtained between lattice-matched Ge and  $\text{Ge}_{0.76}\text{Si}_{0.19}\text{Sn}_{0.05}$  alloy while all other conduction band valleys ( $\Gamma, X$ , etc) are above the  $L$ -valley band

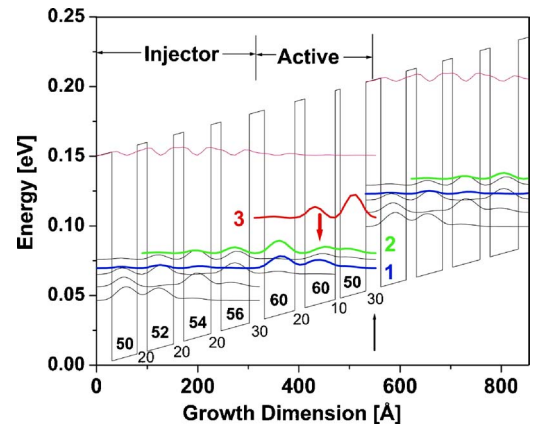


FIG. 2. (Color online)  $L$ -valley conduction band profile and squared envelope functions under an electric field of 10 kV/cm. Layer thicknesses in angstrom are marked with bold numbers for Ge QWs and regular for  $\text{Ge}_{0.76}\text{Si}_{0.19}\text{Sn}_{0.05}$  barriers. Array marks the injection barrier.

edge of the  $\text{Ge}_{0.76}\text{Si}_{0.19}\text{Sn}_{0.05}$  barrier. This band alignment presents a desirable alloy composition from which a QCL operating at  $L$  valleys can be designed using Ge as QWs and  $\text{Ge}_{0.76}\text{Si}_{0.19}\text{Sn}_{0.05}$  as barriers without the complexity arising from other energy valleys.

Figure 2 shows the QCL structure based upon  $\text{Ge}/\text{Ge}_{0.76}\text{Si}_{0.19}\text{Sn}_{0.05}$  QWs. Only  $L$ -valley conduction band lineups are shown in the potential diagram under an applied electric field of 10 kV/cm. In order to solve the Schrödinger equation to yield subbands and their associated envelope functions, it is necessary to determine the effective mass  $m_z$  along the (001) growth direction ( $z$ ) within the constant-energy ellipsoids at the  $L$  valleys along the (111) direction which is tilted with respect to (001). Using the  $L$ -valley principal transverse effective mass  $m_t = 0.08m_o$  and the longitudinal effective mass  $m_l = 1.60m_o$ , we obtain  $m_z = (2/3m_t + 1/3m_l)^{-1} = 0.12m_o$  where  $m_o$  is the free electron mass. The squared magnitudes of all envelope functions are plotted at energy positions of their associated subbands. As shown in Fig. 2, each period of the QCL has an active region for lasing emission and an injector region for carrier transport. These two regions are separated by a 30 Å barrier. The active region is constructed with three coupled Ge QWs that give rise to three subbands marked 1, 2, and 3. The lasing transition at the wavelength of 49  $\mu\text{m}$  is between the upper laser state 3 and the lower laser state 2. The injector region consists of four Ge QWs of decreasing well widths all separated by 20 Å  $\text{Ge}_{0.76}\text{Si}_{0.19}\text{Sn}_{0.05}$  barriers. The depopulation of lower state 2 is through scattering to state 1 and to the miniband downstream formed in the injector region. These scattering processes are rather fast because of the strong overlap between the involved states. Another miniband in the injector region formed of quasibound states is situated 45 meV above the upper laser state 3, effectively preventing escape of electrons from upper laser state 3 into the injector region.

The nonradiative transition rates between different subbands in such a low-doped nonpolar material system with low injection current should be dominated by deformation-potential scattering of nonpolar optical and acoustic phonons. Because of the large energy separation between  $L$  and  $\Gamma$  valleys, and between  $L$  and  $X$  valleys, the  $L$ - $\Gamma$  and  $L$ - $X$  intervalley scattering processes are negligible. Between the four equivalent  $L$  valleys, it can be argued through the matrix element for electron-phonon interaction that the inter

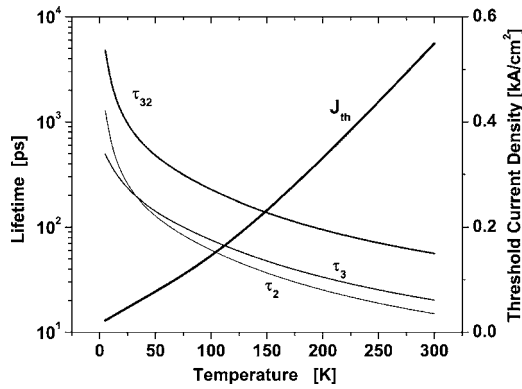


FIG. 3. Lifetimes and threshold current density as a function of operating temperature.

$L$ -valley scattering, an umklapp process, is much weaker than the intra- $L$ -valley scattering. The lifetimes are therefore determined by the intra- $L$ -valley scattering. For this Ge-rich structure, we have used bulk-Ge phonons for calculation of the scattering rate to yield lifetimes for the upper laser state  $\tau_3$  and the lower laser state  $\tau_2$ , as well as the  $3 \rightarrow 2$  scattering time  $\tau_{32}$ .<sup>18</sup> They are shown in Fig. 3 as a function of operating temperature. These lifetimes are at least one order of magnitude longer than those of III-V QCLs owing to the nonpolar nature of GeSiSn alloys. The necessary condition for population inversion  $\tau_{32} > \tau_2$  is satisfied throughout the temperature range. Using these predetermined lifetimes in the population rate equation under current injection:

$$\begin{cases} \frac{\partial N_3}{\partial t} = \frac{\eta J}{e} - \frac{N_3 - \bar{N}_3}{\tau_3}, \\ \frac{\partial N_2}{\partial t} = \frac{N_3 - \bar{N}_3}{\tau_{32}} - \frac{N_2 - \bar{N}_2}{\tau_2}, \end{cases} \quad (2)$$

where  $e$  is the electron charge,  $N_i (i=2,3)$  is the area carrier density per period in subband  $i$  under injected current density  $J$  with an injection efficiency  $\eta$ , and  $\bar{N}_i$  is the area carrier density per period due to thermal excitation of  $n$  doping. Solving the above rate equation at steady state yields population inversion

$$N_3 - N_2 = \tau_3 \left( 1 - \frac{\tau_2}{\tau_{32}} \right) \frac{\eta J}{e} - (\bar{N}_2 - \bar{N}_3), \quad (3)$$

which can be then used to evaluate the optical gain of the TM-polarized mode as<sup>19</sup>

$$g = \frac{2e^2 \hbar |\langle 3|p_z|2 \rangle|^2}{\varepsilon_0 c n m_z^2 \gamma L_p (\hbar \omega_L)} \left[ \tau_3 \left( 1 - \frac{\tau_2}{\tau_{32}} \right) \frac{\eta J}{e} - (\bar{N}_2 - \bar{N}_3) \right], \quad (4)$$

where  $\varepsilon_0$  is the permittivity in vacuum,  $c$  the speed of light in vacuum,  $\hbar$  the Planck constant, and  $\langle 3|p_z|2 \rangle$  the momentum matrix between the two laser states. Other parameters are as follows: index of refraction  $n=3.97$ , lasing transition energy  $\hbar \omega_L=25$  meV, full width at half maximum  $\gamma=10$  meV, length of one period of the QCL  $L_p=532$  Å, area doping density per period of  $10^{10}/\text{cm}^2$ , and unit injection efficiency  $\eta=1$ .

We have simulated the TM-polarized mode in a QCL structure of 40 periods that is confined by double-Au-plasmon waveguide and obtained near unity optical confinement  $\Gamma \approx 1.0$  and waveguide loss  $\alpha_w=110/\text{cm}$ . Assuming a mirror loss  $\alpha_m=10/\text{cm}$  for a typical cavity length of 1 mm, the threshold current density  $J_{th}$  can be calculated from the balancing relationship,  $\Gamma g_{th} = \alpha_w + \alpha_m$ . The result is shown in Fig. 3 for  $J_{th}$  that ranges from 22 A/cm<sup>2</sup> at 5 K to 550 A/cm<sup>2</sup> at 300 K. These threshold values are lower than those of III-V QCLs as a result of the longer scattering times due to nonpolar optical phonons.

In summary, we propose a Ge/Ge<sub>0.76</sub>Si<sub>0.19</sub>Sn<sub>0.05</sub> QCL that operates at  $L$  valleys of the conduction band. According to our estimation of the band lineup, this particular alloy composition gives a clean conduction band offset of 150 meV at  $L$  valleys with all other energy valleys conveniently out of the way. All QCL layers are lattice matched to a Ge buffer layer on a Si substrate and the entire structure is therefore strain-free. The electron effective mass along the growth direction is much lighter than that of heavy holes bringing a significant improvement in tunneling rates and oscillator strengths. The lasing wavelength of this device is 49  $\mu\text{m}$ . With different GeSiSn alloy compositions that are lattice matched to Ge, QCLs can be tuned to lase at other desired wavelengths. Lifetimes determined from the deformation-potential scattering of nonpolar optical and acoustic phonons are at least an order of magnitude longer than those in III-V QCLs with polar optical phonons, leading to a reduction in threshold current density and the possibility of room temperature operation.

This work is supported in part by the Air Force Office of Scientific Research.

- <sup>1</sup>G. Sun, L. Friedman, and R. A. Soref, Appl. Phys. Lett. **66**, 3425 (1995).
- <sup>2</sup>G. Dehlinger, L. Diehl, U. Gennser, H. Sigg, J. Faist, K. Ensslin, D. Grützmacher, and E. Müller, Science **290**, 2277 (2000).
- <sup>3</sup>I. Bormann, K. Brunner, S. Hackenbuchner, G. Abstraiter, S. Schmult, and W. Wegscheider, Appl. Phys. Lett. **80**, 2260 (2002).
- <sup>4</sup>S. A. Lynch, R. Bates, D. J. Paul, D. J. Norris, A. G. Cullis, Z. Ikonjić, R. W. Kelsall, P. Harrison, D. D. Arnone, and C. R. Pidgeon, Appl. Phys. Lett. **81**, 1543 (2002).
- <sup>5</sup>K. Driscoll and R. Paiella, Appl. Phys. Lett. **89**, 191110 (2006).
- <sup>6</sup>R. A. Soref and C. H. Perry, J. Appl. Phys. **69**, 539 (1991).
- <sup>7</sup>D. W. Jenkins and J. D. Dow, Phys. Rev. B **36**, 7994 (1987).
- <sup>8</sup>G. He and H. A. Atwater, Phys. Rev. Lett. **79**, 1937 (1997).
- <sup>9</sup>J. Menéndez and J. Kouvetakis, Appl. Phys. Lett. **85**, 1175 (2004).
- <sup>10</sup>M. Bauer, C. Ritter, P. A. Crozier, J. Ren, J. Menéndez, G. Wolf, and J. Kouvetakis, Appl. Phys. Lett. **83**, 2163 (2003).
- <sup>11</sup>M. A. Wistey, Y.-Y. Fang, J. Tolle, A. V. G. Chizmeshya, and J. Kouvetakis, Appl. Phys. Lett. **90**, 082108 (2007).
- <sup>12</sup>M. Jaros, Phys. Rev. B **37**, 7112 (1988).
- <sup>13</sup>C. G. Van de Walle, Phys. Rev. B **39**, 1871 (1989).
- <sup>14</sup>V. R. D'Costa, C. S. Cook, A. G. Birdwell, C. L. Littler, M. Canonico, S. Zollner, J. Kouvetakis, and J. Menendez, Phys. Rev. B **73**, 125207 (2006).
- <sup>15</sup>V. R. D'Costa, C. S. Cook, J. Menendez, J. Tolle, J. Kouvetakis, and S. Zollner, Solid State Commun. **138**, 309 (2006).
- <sup>16</sup>J. Weber and M. I. Alonso, Phys. Rev. B **40**, 5683 (1989).
- <sup>17</sup>M. L. Cohen and T. K. Bergstresser, Phys. Rev. **141**, 789 (1966).
- <sup>18</sup>B. K. Ridley, *Electrons and Phonons in semiconductor Multiplayers*, 1st ed. (Cambridge University Press, Cambridge, 1997), Chap. 1, p. 15.
- <sup>19</sup>S. K. Chun and K. L. Wang, Phys. Rev. B **46**, 7682 (1992).